8

Application to a case study: the Osormort Viaduct

8.1 Introduction

The second application presented in this thesis focuses on implementing the smart system in a built under-deck cable-stayed viaduct. Therefore, the objective of this chapter is to theoretically study how the behavior of an under-deck cable-stayed bridge would be influenced by the utilization of the smart system.

The Osormort viaduct has been selected as the case study. As it will be explained, its characteristics make it an ideal structure for evaluating the benefits of integrating the smart technology into a real bridge. Since the Osormort viaduct is a prestressed concrete bridge, this chapter takes into consideration certain aspects that were not previously addressed.

To gain insights into the structural behavior of the viaduct, a numerical analysis is performed. The obtained results are subsequently compared and validated with the results provided by the viaduct designers, as documented in the project reports [91]. Then, this chapter explores the performance of the viaduct when equipped with the smart technology. An optimization analysis is conducted to assess the advantages of implementing the smart system in comparison to the reference bridge. The provide a comprehensive evaluation, both cost and CO_2 emissions are taken into account.

8.2 Case study: the Osormort Viaduct

8.2.1 Viaduct configuration

The Osormort viaduct was designed by the Spanish firm Carlos Fernandez Casado S. L. in 1993. The principal designer was Javier Manterola (1936-), a renowned Spanish civil engineer and professor of bridges at the Civil Engineer School of the Universidad Politécnica de Madrid. Manterola is very well-know for some landmark projects as the Barrios de Luna cable-stayed bridge, the Euskalduna bridge in Bilbao and the Puente de la Constitución de 1812 cable-stayed bridge in Cadiz. Manterola has received multiple professional awards, such as the "Prince of Viana Award for Culture" in 2005 or the "National Engineering Award" from the Ministry of Development in 2001 [92].

The Osormort viaduct (Figure 8.1) was constructed by Agroman S.A and officially inaugurated in 1997. It is located in Sant Sadurní d'Osormort (Catalonia, Spain) and serves as a crucial link for the transversal axis of Catalonia (Highway C-25), allowing to cross the Riera Major stream and road BV-5201. In 2013, a second viaduct was built parallel to the original, in order to split both traffic directions.

The Osormort viaduct has a total length of 504 meters and a plan radius of 1550 meters, with a maximum height above ground of 30 meters (see Figures 8.2a and 8.2b). It is a continuous viaduct with 13 spans. The end spans have a length of 32 meters, while the remaining 11 have a span length of 40 meters. The deck cross-section is a double-triangular lightened slab. It has a total width of 13.20 meters (with 12.00 available for traffic) and a depth of 1.6 meters (see Figure 8.2c).

The prestressed concrete deck is complemented with an under-deck cable-stayed system. The cable-stayed system has a rise (f) of 4.8 m in the end spans and 6.0 m in the remaining ones, resulting in a rise-to-span ratio of $f/L = 0.15$ in both cases. The strut is materialized by a triangular steel cell (see Figure 8.1, top right) where the elements have a square hollow cross-section with dimensions 320 x 320 x 20 mm.

The connection between the cables and the struts is achieved by a steel saddle consisting of three semicircular tubes. Two of these tubes facilitate the deviation of the cables while an extra tube has been incorporated for ease of replacement of any of the cables. At the piers, diaphragms are installed where the cables are anchored.

Figure 8.1: Pictures of the Osormort Viaduct, taken by the author.

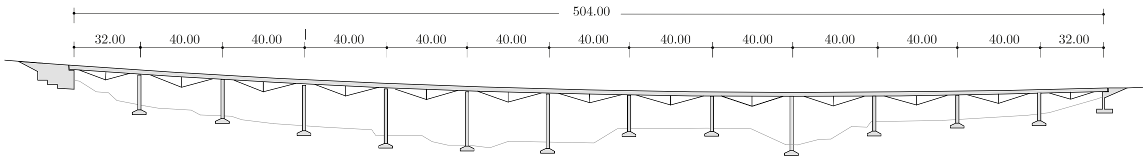

(a) Elevation view.

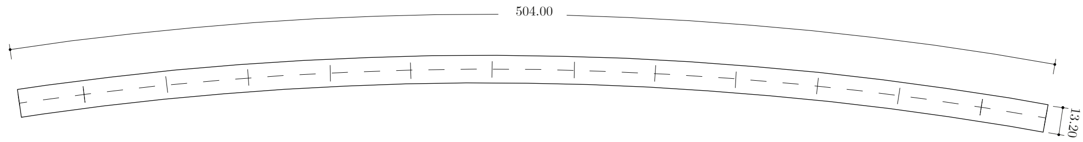

(b) Plan view.

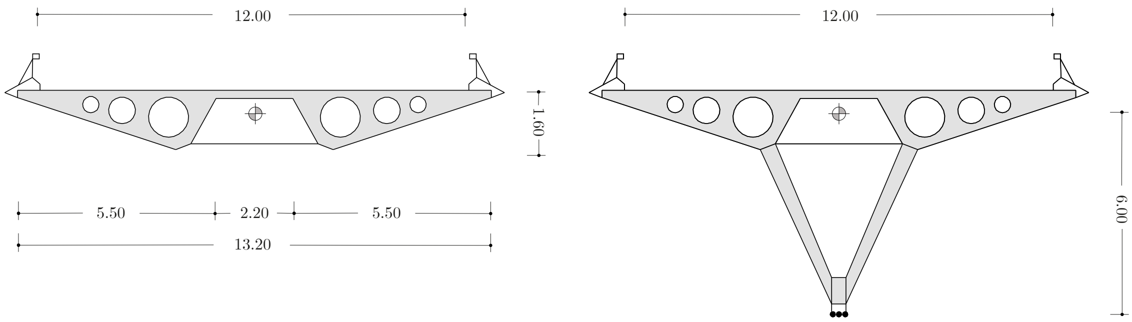

(c) Cross sections at supports and midspan.

Figure 8.2: Drawings of the Osormort Viaduct. All dimensions expressed in meters. Adapted from [91].

As previously mentioned, the contribution of the cable-stayed system in withstanding the permanent loads depends on the initial prestress force. In contrast, its contribution in withstanding live loads depends on the relative stiffness between deck and tendons [4], [14], in other words, the cables serve as intermediate elastic supports for the deck.

The contribution of the cable-stayed system in withstanding the live loads is typically used to classify the type of bridge. The Osormort Viaduct presents an intermediate solution between external prestressing and a cable-stayed system. This approach offers several benefits for medium-span bridges, as outlined in the Osormort project report [91]. To point out the most relevant:

- Unlike conventional cable-stayed bridges, there is no need to widen the deck cross-section to accommodate tendon anchorages.
- Compared to a conventional prestressing located within the section depth, this system is much more efficient, as it significantly increases the eccentricity of the tendons respect to the deck's center of gravity.

- Due to the lower efficiency of the tendons compared to conventional cable-stayed systems, the design is less likely to be conditioned by fatigue-related issues.

8.2.2 Design basis

Materials and internal prestressing

The materials for the structural elements of the viaduct have been obtained from the original project drawings and the calculation report [91], generously provided by Carlos Fernandez Casado S.L. The deck was built using a HA-40 concrete, which has a characteristic compressive strength of $f_{ck} = 40$ MPa and an elastic modulus of $E_c = 38000$ MPa. The struts and deviators are made from A-52 steel, which has a yield strength of $f_{sy} = 355$ MPa and an elastic modulus of $E_s = 210000$ MPa.

The cable-stayed system is composed by two cables with 32 strands each for the 40-meter spans and two cables with 27 strands each for the 32-meter spans. Each strand has a size of 0.6” and an area of 150 mm^2. According to the calculation report, the cables of the Osormort Viaduct were designed to work at 55% of their breaking strength. This value falls between the typical range of 45% for cable-stayed bridges and 60% for extradosed and externally post-tensioned bridges, showing how the Osormort Viaduct lies between these two structural typologies of bridges. Furthermore, it has been verified that the load oscillations caused a stress variation in the cable-stayed system below 100 MPa, which is a common acceptable value in prestressed systems.

Regarding the internal prestressing, the drawings (see Figure 8.3) indicate that all tendons are units of 19 strands, leading to a tendon area of 2850 mm^2. These tendons have been prestressed at 3850 kN, which corresponds to 75% of their breaking strength. Furthermore, an elastic modulus of $E'_s = 190000$ MPa has been considered. Each span has ten tendons, which are aligned with the beginning and the end of each construction phase (detailed in Section 8.2.3). The tendon layout varies along the depth of the cross-section to optimize its effect. This is shown in Figure 8.3, which illustrates the specific layout used for the more eccentric tendons of the cross-section used in the 40-meter spans (tendon no. 6). Additionally, the pier diaphragms are reinforced with a transversal prestressing.

The partial factors for the reduction of the strength of the materials are $\gamma_c = 1.50$ for concrete and $\gamma_s = 1.15$ for steel.

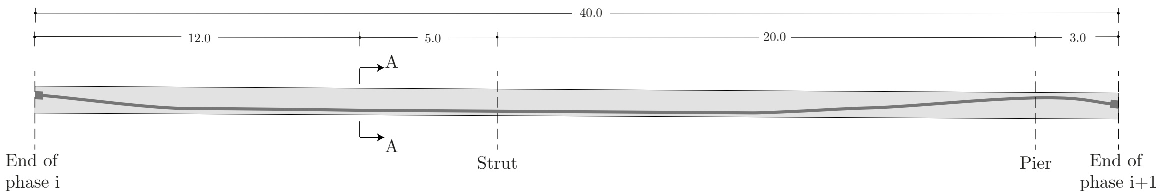

(a) Elevation view of tendon no. 6.

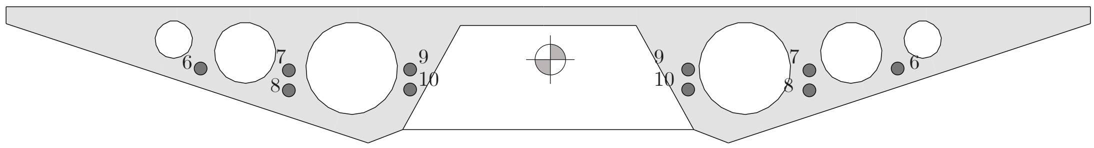

(b) Position of the internal prestressing at section A-A.

Figure 8.3: Internal prestressing layout for an intermediate construction phase. All dimensions expressed in meters. Adapted from [91].

Loads and load combinations

The loads considered in the calculations can be classified in two main groups. The first group corresponds to the permanent loads, and it integrates the following:

- Self-weight. It is estimated considering the real geometry of the viaduct and the unit weight of each material (25 kN/m^3 for concrete and 78.5 kN/m^3 for steel).
- Initial prestressing of the cable-stayed system. According to the calculation report [91], the initial prestress force is determined in order to compensate the dead weight of the viaduct plus an additional 5% at the location of each strut. Section 8.3.2 details the values of these prestressing loads in the original project and how they have been obtained in this work.
- Dead load. The parapet and barrier, according to the calculation report [91], have a total weight of 5.77 kN/m per side. For the pavement, a surface weight of 2 kN/m^2 applied in the width of the bridge available for traffic (i.e., 12 meters) has been considered.

The second group of loads considered in this study are the traffic loads. Other variable loads such as temperature and wind were excluded from the analysis. The reason is that the smart system does not affect the structural behavior of the viaduct when subjected to these loads. Therefore, to account for these loads would not contribute to the comparison with the original viaduct.

The traffic loads were defined according to the Spanish code for bridge actions of 1972 [93], from now on IAP–72. This standard was applicable in Spain at the time of the project's conception in 1993. These loads are the following:

- Uniformly Distributed Load (UDL) of 4 kN/m^2 applied only in the unfavorable parts of the surface available for traffic (12 meters).
- Tandem system (TS) of 600 kN distributed in 3 axles spaced 1.5 meters. The TS is considered to be in its most unfavorable position.

To validate the calculation model and analyze the structural behavior of the viaduct, the IAP–72 is applied. On the other hand, when applying the smart system, the current Eurocodes are used, considering the Spanish National Annexes when necessary. In order to make a comparison between the smart solution and the conventional structure, the latter was also analyzed using the Eurocodes to ensure consistency in the analysis.

According to the current Eurocodes [78], the traffic loads are the following:

- Uniformly distributed load (UDL system) of 9 kN/m^2 in a width of 3 meters and 2.5 kN/m^2 in the remaining width available for traffic (9 meters).
- Three tandem systems (TS) of 600 kN, 400 kN and 200 kN each, distributed in 2 axles spaced 1.2 meters. These TS are considered to be in their most unfavorable position.

During the conception of the viaduct, the applicable code for structural concrete was the Spanish norm of 1991 [94], from now on EH–91. The applicable limit states in the deck and the cable-stayed system are Ultimate Limit State (ULS) and different Serviceability Limit States (SLS), which are the rare or characteristic, frequent and quasi permanent load combinations.

The EH–91 defines the different load combinations and their load factors for verifying these limit states. For permanent loads, an unfavorable effect is increased by a factor of $\gamma_f = 1.50$, with intense execution control. In contrast, a favorable effect is decreased by a factor of $\gamma_f = 0.90$. When it comes to variable loads, an unfavorable effect is increased by a factor of $\gamma_f = 1.50$, while a favorable effect is neglected. These factors correspond to ULS verifications, as for SLS verifications all factors are equal to 1.0. The combination factors for the traffic loads (to be considered in specific limit states) are $\Psi_{1,q} = 0.75$ for the TS and $\Psi_{1,Q} = 0.4$ for the UDL.

It is noted that, in this case, the values of γ_f in ULS according to the EH–91 are more restrictive than those of the actual Eurocodes ($\gamma_f = 1.35/1.00$ for permanent actions and $\gamma_f = 1.35/0.00$ traffic loads).

Finally, in this research, the Fatigue Load Model 1 of the Eurocodes has been adopted for fatigue verifications in the cable-stayed system. Fatigue Load Model 1 follows the configuration of the considered characteristic Load Model, and applies the following factors to TS and UDL: $0.7Q_{ik}$ and $0.3q_{ik}$, respectively.

8.2.3 Construction process

The selection of a typical span length of 40 meters for the viaduct was based on the decision of adopting a movable scaffolding system [20] for the construction. This building method allows each span to be supported only on the piers, without the need for any additional ground-based support.

The construction process consists in building the viaduct span-by-span (see Figure 8.4). Each construction phase ends with a cantilever of 3 meters (measured from the pier axis), equivalent to 7.5% of the span length. In continuous bridges, this distance would normally be around 20-25% of the span, but in this case, it was significantly smaller due to the change in bending moments caused by the under-deck cable-stayed system.

For the construction of the following span, the scaffolding system is supported in the cantilever, at a distance of only 1 meter from the pier axis. The front of the scaffolding rests on provisional metal girders supported on the next pier shaft.

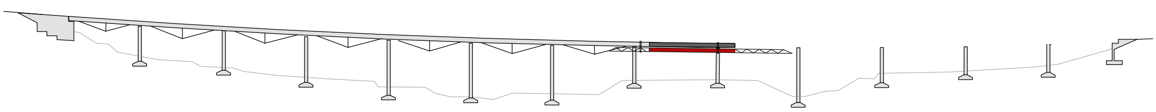

Figure 8.4: Construction phase of an intermediate span.

The under-deck cable-stayed system and the internal prestressing are placed before the concreting and loaded simultaneously before the formwork is removed.

The construction lasted 210 days, with an average of 16.15 days per span.

8.3 Numerical analysis of the Osormort viaduct

8.3.1 Description of the Finite Element Model

To analyze the structural behavior of the Osormort Viaduct a Finite Element Model (FEM) has been developed using SOFiSTiK (Figure 8.5), a commercial FE software for structural analysis. The results obtained from this model are then compared with those provided in the calculation report of the original project [91]. Thus, some of the simplifications made there are also herein reproduced.

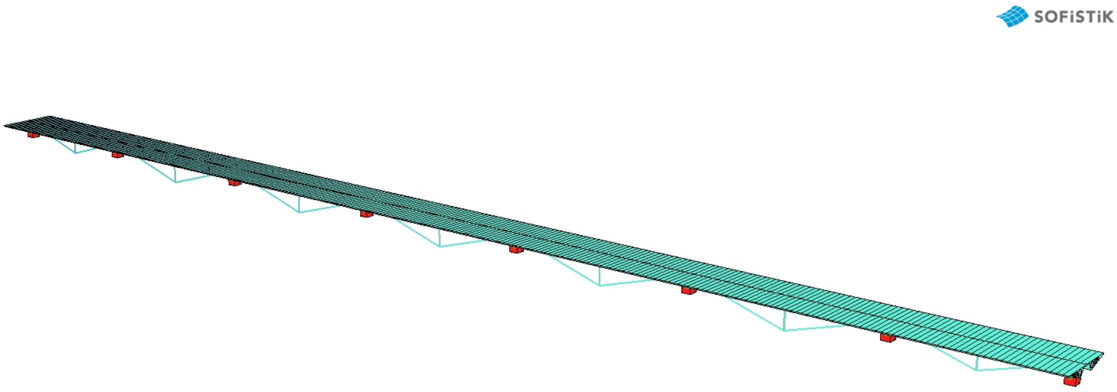

Figure 8.5: Overview of the SOFiSTiK model for the Osormort viaduct.

In the same way as in the original project [91], only seven spans are modeled: two end spans (32 m) and 5 intermediate spans (40 m). Being all the intermediate spans identical, this reduced model is sufficient to obtain a representative characterization of the viaduct. Additionally, this work focuses in the middle span, being representative of almost the whole viaduct.

The FE model reproduces the same geometry, cross-sections and materials as those described in Sections 8.2.1 and 8.2.2. The deck is modeled by consecutive beam elements, each one meter long. All supports are rolled but the one located at the left end, which is a pin support to resist horizontal loads and avoid instabilities. At all supports, rotation around the longitudinal axis of the bridge is constrained to simulate the double bearing. At midspan, each strut is modeled as a simple beam element which connects the deck's center of gravity to the lowest part of the cable-stayed system.

The cable-stayed system is modeled with truss elements, which can only take axial forces. These elements connect the center of gravity of the deck at the supports, with the lower end of the midspan strut.

Concerning the internal prestressing, a simplified approach utilizing a single equivalent tendon has been employed. This equivalent tendon has the same cross-sectional area as that of the ten individual tendons and its layout aligns with the mean center of gravity of the ten individual tendons.

A linear analysis, including both geometrical and material linearity, is performed using SOFiSTiK's beam element formulation, that accounts for shear deformation and hinge behavior. According to Ruiz-Terán and Aparicio [14], these bridge types can be safely analyzed with a linear analysis, because accounting for the non-linearity of the prestressed concrete in ULS would lead to a reduction in the stresses on the deck and an increase in the load carried by the cable, which is primarily governed by SLS design considerations.

The structure is evaluated for time-dependent effects (creep and shrinkage in the concrete and relaxation in the prestressing steel) over a period of 10,000 days.

The loads applied to the model are those described in Section 8.2.2. These loads are combined with their corresponding factors, defined in the same section, to obtain the combinations at ULS and SLS.

8.3.2 Results and model validation

Permanent state

The initial prestressing has to be established to determine the permanent state. Completely compensating the permanent loads at the points where the prestressing force is introduced (i.e. achieve zero deflection at the anchorage positions) is a standard practice in cable-stayed bridges, as it allows to subdivide the main span in multiple sub-spans for this loading scenario [14], [95]. Strasky [96] emphasized the importance of balancing the permanent loads at the deviators. By ensuring that the permanent loads, in combination with the initial prestress, results in zero deflections at these points, it becomes feasible to prevent any stress redistribution caused by long-term effects at these locations. This is possible because in the locations where there is no initial deflection, the long-term effects will only introduce axial forces on the deck.

However, the compensating criterion is a designer's choice and in this particular case, a different approach was taken. The cable-stayed system is prestressed enough to compensate at midspan (strut location) the self-weight of the deck increased by a 5%, as indicated in the calculation report [91]. Based on the loads described in Section 8.2.2, the self-weight accounts for roughly 83% of the permanent loads. Therefore, compensating for the dead weight plus the additional 5%, results in a compensation of approximately 87% of the permanent loads.

To achieve comparable results, the same approach is employed in the calculations of this study. Table 8.1 presents a comparison of the axial forces in the stays for the self-weight multiplied by a factor of 1.05 plus the initial prestressing of the cable-stayed system, in the original calculation report [91] and in this study. The table shows that the differences between the two sets of results are small, indicating a good accuracy of the finite element model.

Table 8.1 Axial forces in the stays for the self-weight of the deck increased by a 5%, plus the initial prestressing of the cables. Values expressed in kN.

Span	Values obtained from the original project [91]	Values obtained from the FE Model
1	5647	5675
2	6594	6741
3	6440	6585
4	6434	6575
5	6440	6585
6	6594	6742
7	5647	5676

These forces could also be obtained analytically, using the expressions proposed by Ruiz-Terán [4] and indicated in Equation 4.1. In this case, the adimensional parameter ρ (portion of the self-weight compensated by the external cable-stayed system) is set to 1.05. The deck has a self-weight of $g = 180$ kN/m, resulting in a value of $R_g = 3780$ kN for the 40-meter spans and $R_g = 3024$ kN for the 32-meter spans. By force equilibrium and considering the rise of the cable-stayed system, the axial force in the stays results in $N_g = 6577$ kN for the 40-meter spans and $N_g = 5262$ kN for the 32-meter spans, similar values to the results shown in Table 8.1.

Once the initial prestressing in the cable-stayed system is determined, it is introduced in the numerical simulation considering the span-by-span construction process. The axial forces in the stays once the construction is completed are shown in Table 8.2. Specifically, the axial forces in the cable-stayed system for the permanent state (self-weight + dead load + initial prestressing of the stays + internal prestressing) after completing the structure (without time-dependent effects) are compared with those obtained after after 10,000 days (with time-dependent effects). Therefore, the second set of results accounts for the permanent state plus the long-term effects on the structure.

Table 8.2 Axial forces in the stays for the permanent state. Values expressed in kN.

Span	After completing the structure (without time-dependent effects)	After 10,000 days (with time-dependent effects)
1	5014	4167
2	5899	5059
3	5762	4891
4	5757	4892
5	5756	4883
6	5960	5144
7	4860	3837

As these results prove, the long-term effects in these type of bridges cause an increase of bending in the deck and a reduction of the axial forces in the stays. According to Ruiz-Terán and Aparicio [97], this effect is particularly significant in continuous bridges if compared to single-span bridges with under-deck cable-stayed systems. Consequently, the beneficial effect of the initial load compensation is reduced over time. This important effect is graphically shown in Figure 8.6, which plots the bending moment distribution in the deck due to permanent loads (in this case without the effect of the internal prestressing) at the end of the construction (blue) and after 10,000 days (red).

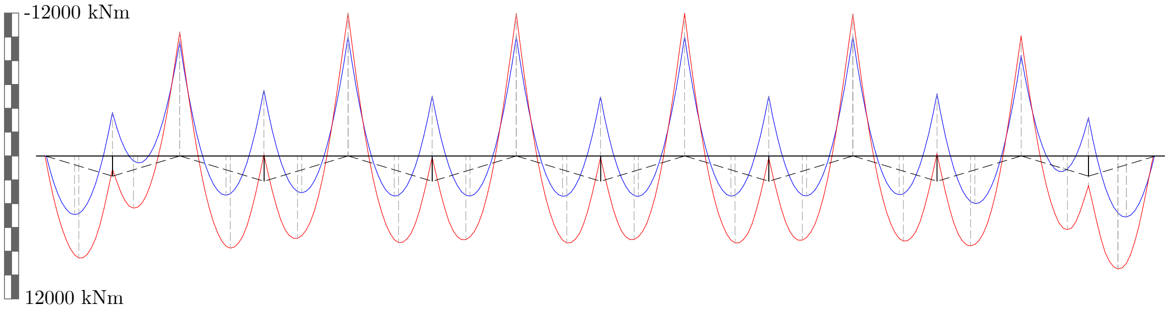

Figure 8.6: Bending moment distribution in the deck due to permanent loads (without the effect of the internal prestressing). At the end of the construction (blue) and after 10,000 days (red).

This decrease of the cable axial force represents a relevant drawback of the cable-stayed system, as it strongly reduces the efficiency of the cable-stayed system. Although this will be addressed in Section 8.4.1, this effect can be compensated by using a smart system, as the cables can be stressed at any point during the service life of the structure.

Considerations on the construction process

In extradosed and cable-stayed bridges, the permanent state is highly dependent on the construction sequence [25]. Consequently, to obtain the real stress state due to the permanent loads, the construction process of the viaduct has been modeled span-by-span, as illustrated in Figure 8.7.

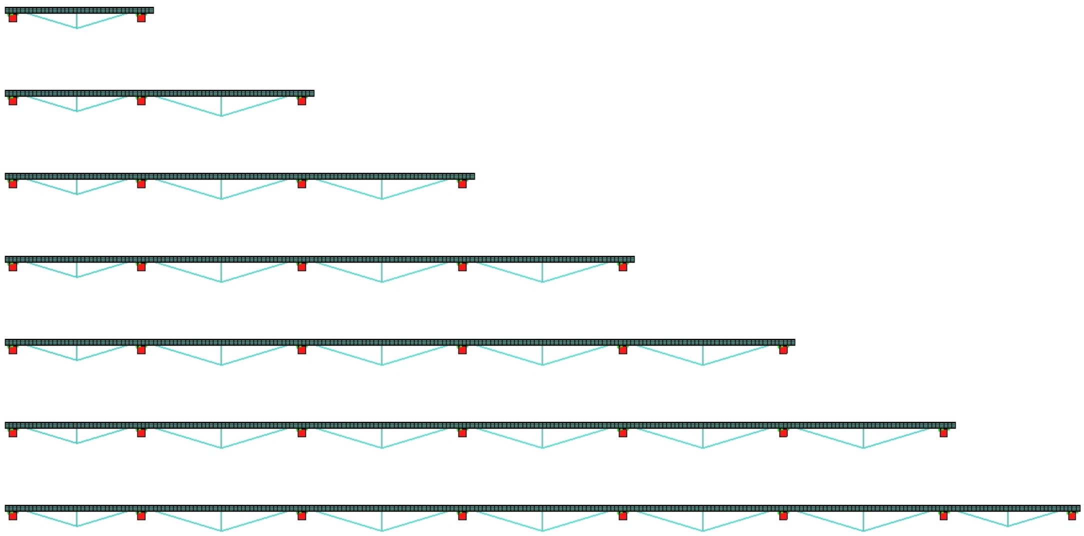

Figure 8.7: Construction sequence considered in the reduced 7-span FEM for the Osormort viaduct.

The construction phases have been determined according to Section 8.2.3. These phases include the application and removal of the construction loads in each phase. Once each phase is completed (i.e., deck built up to the pier axis plus an additional cantilever of 3 meters), the subsequent construction stage corresponds to the weight of the scaffolding and concrete pouring, which is applied as a point load at a distance of 1 meter from the pier axis. The magnitudes of these loads have been obtained from the original calculation report [91]. They are 5257 kN for the first six spans and 3931 kN for the last span.

The results from the FEM show interesting findings in relation to the bending moment distribution caused by the statically indeterminate part of the prestressing. Figure 8.8 shows this distribution considering the adopted construction sequence (red) and in the hypothesis that all spans were built simultaneously (blue). It can be observed how the bending moment distribution is reduced an average of 25% if the construction process is taken into account in the numerical model, proving the importance of its consideration.

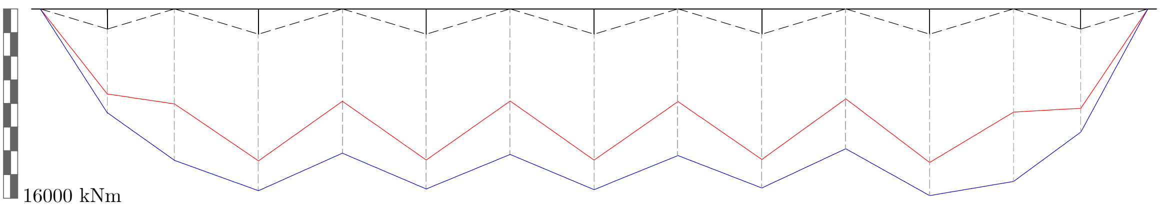

Figure 8.8: Bending moment distribution in the deck due to the statically indeterminate part of the prestressing. Considering the adopted construction process (red) and considering all spans to be built simultaneously (blue).

Efficiency of the cable-stayed system

Next, the contribution of the cable-stayed system in withstanding live loads is examined. To this end, two parameters, described in the previous chapters, are employed. These parameters are the live load distribution ratio (β_Q), obtained as the axial load in the strut due to live load (R_Q) over the total live load, and the efficiency of the cable-stayed system (ξ), calculated as expressed in Equation 2.1. These parameters depend on the relative stiffness between the deck and the cables, the support conditions and the type of applied load.

To determine the values of ξ and β_Q a unitary load is applied to the structure modeled in the FEM. Two types of loads are considered: a point load applied at midspan of span 4 and a uniformly distributed load applied at span 4. The relevance of the support conditions is also investigated by repeating the analysis on the same bridge, but without continuity at the pier sections (equivalent to a simply supported span). The results of these analyses are presented in Table 8.3.

Table 8.3 Load distribution ratio (β_Q) and efficiency of the cable-stayed system (ξ).

	Point load at midspan	**Uniformly distributed load**
For the 7-span model (continuous bridge)		
β_Q	16 %	10 %
ξ at midspan	18 %	25 %
ξ at pier	13 %	11 %
For a modified model (simply-supported independent spans)		
β_Q	28 %	17 %
ξ at midspan	28 %	35 %

Table 8.3 demonstrates the relevance of both the type of load and support conditions on the distribution of the live load. The obtained values are consistent with the findings of Ruiz-Terán and Aparicio [4], [15], [97]. In fact, according to these studies, under-deck cable-staying systems are not recommended for continuous bridges due to their inefficiency under live loads.

While these systems are able to successfully compensate the permanent load, they are not effective in handling hogging bending moments in the support sections over the piers, where the cable-stayed system lacks eccentricity. Moreover, the reduction of sagging bending moment achieved with the cable-stayed system is less than that of a simply supported structure. To address these issues, Ruiz-Terán and Aparicio [97] propose two potential solutions: breaking the continuity between spans to create highly-efficient independent simply-supported spans or implementing a combined cable-stayed system (cable above and below the deck).

The low values of β_Q indicate that the Osormort viaduct should be classified as an external post-tensioned bridge rather than a cable-stayed bridge. However, the term is still used as it was the name used by the designers. Furthermore, the smart system introduced in the next section enables the cables to resist a significant portion of the live load, thereby making the term applicable.

Finally, Figure 8.9 illustrates the bending moment envelopes in span 4 resulting from the traffic live load, as specified by the IAP–72. The envelope has been obtained for the Osormort bridge (in red) and for an equivalent bridge without the cable-stayed system (in blue). By comparing the two envelopes, it can be observed that the cable-stayed system provides a minor contribution in withstanding live loads, specifically near the supports.

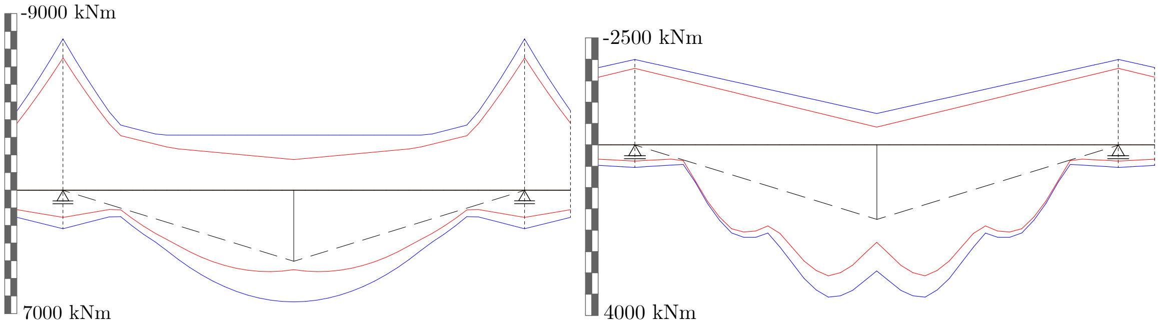

(a) Uniformly distributed load (4 kN/m^2). **(b)** Tandem system (600 kN).

Figure 8.9: Bending moment envelopes in span 4 due to traffic live load, according to the IAP–72. Bridge with (red) and without (blue) under-deck cable-stayed system.

Results at SLS and ULS

A summary of the verifications performed for the Osormort viaduct is provided, considering the results obtained from the FEM for the deck and stays in span 4. These verifications are performed in accordance with the construction standards applicable at the time of construction (IAP–72 and EH–91). Two scenarios are considered: with and without time-dependent effects.

The limit states to verify in the stay cables are the following:

- The maximum stress (σ_{max}) at SLS (characteristic combination) should verify: $\sigma_{max} \leq 0.55\ f_{pu}$. In this case: 663 MPa $\leq$ 990 MPa.
- The maximum stress variation ($\Delta\sigma_{max}$) due to the live load should not exceed 100 MPa. In this case: $\Delta\sigma_{max} = 54$ MPa $\leq$ 100MPa

These verifications, as considered in the original project [91], are based on the limitations provided by the codes for external post-tensioning. If the criteria for cable-stayed system were used, the maximum stress variation could be significantly increased, but the anchorages would be considerably more expensive. Additionally, the maximum stress would be limited to 45% of the breaking strength. To ensure consistency in the comparison of results, the same criteria adopted in the original project [91] are used for the verification of the smart system described in the next section.

Regarding the internally prestressed concrete deck, the following verifications are performed:

- Maximum utilization factor (UF) for bending at ULS: UF $= 0.9 \leq 1$.
- Verification of the decompression limit state (at quasi permanent SLS combination). The minimum stress in the concrete is: $\sigma_{c,min} = 0.2$ MPa ≥ 0 MPa, verifying that the concrete is always in compression.
- Verification of the maximum crack width (w_k) for the frequent SLS combination. It is verified that the maximum crack does not exceed the limitation for the corresponding exposure conditions: $w_k \leq w_{max} = 0.20$ mm.
- Verification of the maximum compressive stress ($\sigma_c \leq 0.6\ f_{ck}$) under the characteristic SLS combination: $\sigma_c = 15.9$ MPa ≤ 24 MPa.

8.4 Application of the smart system to the Osormort Viaduct

8.4.1 Working principles of a partially smart system

This section describes the implementation of a smart system on the Osormort viaduct, with the goal of improving the efficiency of the cable-stayed system by enabling real-time adjustments of the tension in the stays. The smart behavior is achieved by replacing the midspan struts with linear actuators that can elongate and contract in response to the live load. This is the same technology that has already been described in the previous chapters.

When the actuator elongates, the contribution of the stays in resisting the live load increases rapidly, resulting in real-time improvements to the efficiency of the cable-stayed system. The elongation of the actuator is simulated in the FEM by introducing a strain in the strut along the axial direction.

The same working procedure as described in Section 3.2.1 is followed. Again, the system is designed as partially smart, with the actuator only working if the live load threshold (q_t) is exceeded. To evaluate the effectiveness of the partially smart system, the Osormort viaduct is analyzed by varying the parameter q_t/q_d, from a conventional under-deck cable-stayed system ($q_t/q_d = 1$) to a fully smart cable-stayed system ($q_t/q_d = 0$). Additionally, various intermediate situations are examined to determine the optimal q_t/q_d. Here, q_d refers to the design live load, which corresponds to the TS and the UDL as specified in the codes (see Section 8.2.2).

Moreover, the actuator is used to counteract the loss of tension resulting from long-term effects, which causes an increment in bending moments in the deck. This strategy offers additional possibilities for optimizing the design of the deck.

8.4.2 Comparison of results: conventional vs. smart structure

In this section, the results when using the smart system in the Osormort viaduct are presented and then compared to the ones obtained with the conventional system. These results have been obtained by taking into account the Eurocodes, considering the traffic loads and load combination factors described in Section 8.2.2. Thus, the results are not directly comparable with those shown in Section 8.3.2.

First, the bending moment envelopes resulting from traffic loads (UDL + TS) with and without the influence of the actuator are compared. Figure 8.10 shows three scenarios: i) the structure operating as a conventional under-deck cable-stayed system ($q_t/q_d = 1.0$) (in blue), ii) a partially smart structure with the actuator compensating for half the acting traffic load ($q_t/q_d = 0.5$) (in green), and iii) a fully smart structure with the actuator functioning for any value of the acting traffic loads ($q_t/q_d = 0.0$) (in red).

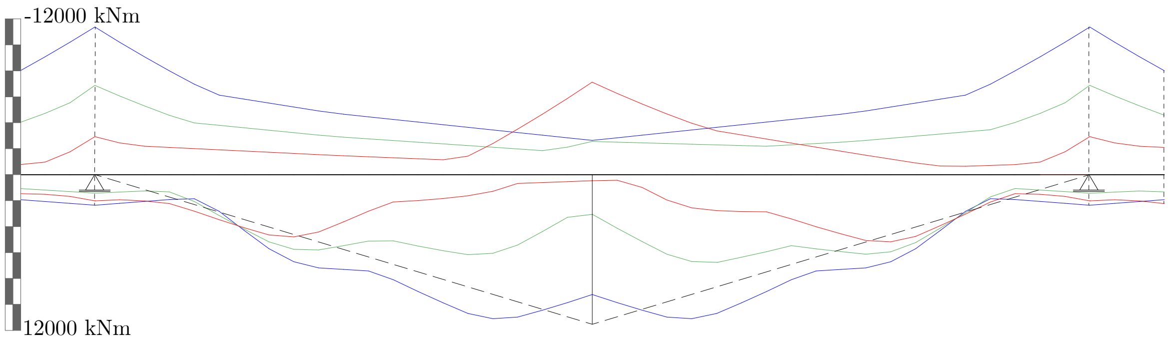

Figure 8.10: Bending moment envelope in span 4 due to traffic loads for $q_t/q_d = 1.0$ (blue), $q_t/q_d = 0.5$ (green) and $q_t/q_d = 0.0$ (red).

Figure 8.10 demonstrates the relevant impact of the smart system on the distribution of bending moments resulting from the live load. The results shed light on the fact that the partially smart strategy, represented by the green curve, achieves optimal outcomes by successfully minimizing the bending moments along the deck. This strategy significantly reduces the hogging bending moments at the supports (previously identified as problematic areas in continuous under-deck cable-stayed bridges) and the sagging bending moments at midspan. These findings suggest that the adoption of a partially smart approach could lead to an optimized deck design, as will be detailed in Section 8.4.3.

Next, the verifications at ULS and SLS described in Section 8.3.2 have been performed for the smart Osormort viaduct, for values of q_t/q_d from 0 (fully smart structure) to 1 (conventional structure). The results are shown in Table 8.4.

Table 8.4 ULS and SLS verifications for the smart Osormort viaduct.

Degree of responsiveness ($\mathbf{q_t/q_d}$)	**0.00**	**0.25**	**0.50**	**0.75**	**1.00**
Verifications of the concrete deck					
Max utilization factor at ULS: UF [-]	0.5	0.6	0.6	0.7	0.9
Min. comp. stress at $SLS_{qua.perm.}$: $\sigma_{c,min}$ [MPa]	0.1	0.1	0.1	0.1	1.1
Max. comp. stress at $SLS_{char.}$: $\sigma_{c,max}$ [MPa]	18.9	16.5	15.5	16.0	16.6
Verifications of the cable-stayed system					
Max. stress at SLS: σ_{max} [MPa]	1055	963	870	777	685
Max. stress variation: $\Delta\sigma_{max}$ [MPa]	226	178	130	83	35

First, the deck verifications are discussed. As the value of q_t/q_d decreases, the ultimate limit state utilization factor (UF) is reduced and the maximum compression stress in the characteristic SLS combination increases. This is attributed to the fact that the cable-stayed system withstands a greater portion of the live load, thereby reducing the demand for the flexural response of the deck. This also results in greater compression in the deck caused by the increased force in the stays.

The minimum compression stress for the quasi-permanent SLS combination remains constant across all smart cases, as the traffic live load does not factor into this combination. This value differs in the conventional bridge ($q_t/q_d = 1.0$), since in the remaining cases the actuator is elongated to counteract part of the loss of tension due to long-term effects. It is observed that in this case study, since the only considered variable loads are the traffic loads, the quasi-permanent load combination corresponds to the permanent state plus the long-term effects. Furthermore, the crack width requirement for the frequent serviceability limit state is satisfied in all scenarios.

Regarding the stays, as the q_t/q_d ratio decreases, the stress in the cable-stayed system rises due to its greater efficiency. However, for high values of q_t/q_d, the requirements are not fulfilled (indicated in red), suggesting the need for a larger cross-sectional area of the stays.

Consequently, to apply the smart system, it is necessary to find an optimal solution that balances reducing the deck's height and internal prestressing with increasing the area of the stays. In the following section, various optimization strategies are proposed to achieve an optimum design.

8.4.3 Optimization of the deck

Optimization strategies

As demonstrated in the previous Section 8.4.2, a smart system can be employed to optimize the design of the deck, leading to potential material and cost savings. With this aim, two optimization strategies are proposed: i) decreasing the deck height ($h = 1.6$ m in the reference bridge), resulting in a smaller cross-sectional area of the deck, and ii) reducing the internal prestressing, which currently consists of 10 tendons of 19 strands each. In contrast, the use of a smart system will result in an increase of the cross-sectional area of the cable-stayed system, as the axial force carried by the stays raises.

In order to determine the optimum operation level of the smart system, various values of q_t/q_d are tested, ranging from 0 to 1, through the optimization process. All the remaining parameters, including geometry and materials, are kept constant. The bridge deck is optimized to achieve a utilization factor of $UF = 0.9$ while satisfying all remaining verifications of the deck and the cable-stayed system. The value of $UF = 0.9$ has been selected to match the UF obtained in the previous section (see Table 8.4) for the conventional viaduct, enabling a valid comparison. Other design criteria, such as the ratio of the permanent loads compensated by the initial prestressing of the stays (ρ), remains unchanged.

It is noted that due to the numerous variables involved in the design of the viaduct and how they impact each limit state differently, a formal optimization approach was not pursued. Instead, an approximate optimization method was employed, varying the values of the three parameters previously indicated (deck height, area of the internal prestressing and area of the cable-stayed system), until the most cost-effective solution is achieved. This approach provides a practical solution to the design problem. As a simplification, the optimization is only performed for span 4, a typical intermediate span (40 meters), and then it is extrapolated to the remaining spans.

The optimization objective is to minimize the overall cost of the viaduct by considering the costs of the concrete deck, internal prestressing, cable-stayed system, actuator and energy consumption required for operation. Moreover, the carbon footprint of each scenario, expressed in units of equivalent kg of CO_2, is evaluated. Table 8.5 presents the unitary cost and carbon emissions of each unit.

Table 8.5 Unitary costs and carbon emissions for the units of the viaduct considered in the optimization.

Unit	Cost	ECC
HA-40 concrete	109 €/m^3	0.16 kg CO_2e/kg
Prestressing steel	3 €/kg	2.60 kg CO_2e/kg
Actuator	1840 €/unit	5580 kg CO_2e/unit
Operational energy	0.08 €/kWh	0.265 kg CO_2e/kWh

To calculate the overall cost and carbon footprint of the deck, the values obtained for each material are multiplied by their corresponding quantities. The pricing information for the actuator has been provided by a manufacturer and corresponds to a hydraulic actuator with a capacity of 1000 kN. The cost of the actuator is assumed to vary linearly based on the required force for each case. The costs associated with the sensors and other electronic equipment are not included in the current analysis due to limitations in available data and their relatively low price compared to the aforementioned units.

To calculate the operational energy required by the actuator over the service life of the viaduct, the number of working hours is determined for the different values of q_t/q_d. To achieve this, the probability of the design load being exceeded by a certain percentage over the service life of the structure is taken into account, in accordance with the guidelines set out in the Eurocodes [77] and as described in Chapter 6.

Results

Considering the above, four viaducts are designed for varying degrees of responsiveness. Table 8.6 provides a summary of the resulting dimensions. The dimensions shown for $q_t/q_d = 1.00$ correspond to the Osormort viaduct and are provided for comparison purposes.

Table 8.6 Dimensions of the optimized smart Osormort viaduct.

Degree of responsiveness	**Height of the deck [m]**	**Area of the stays [cm^2]**	**Area of the internal prestressing [cm^2]**
$q_t/q_d = 1.00$	1.6	96	285
$q_t/q_d = 0.75$	1.5	96	171
$q_t/q_d = 0.50$	1.5	138	143
$q_t/q_d = 0.25$	1.5	180	143
$q_t/q_d = 0.00$	1.5	216	143

The following comments are made regarding the optimization process and the resulting dimensions:

- By decreasing the degree of responsiveness, the cable-stayed system carries a greater proportion of the live load. Thus, a larger cross-sectional area is necessary.
- Consequently, the bending moments in the deck are reduced, allowing to reduce the required height of the deck and cross-sectional area of the internal prestressing.
- In the original design, ULS was the conditioning limit state. However, as the dimensions of the deck are reduced (thanks to the effect of the smart system), the quasi-permanent SLS combination becomes more restrictive. Since the permanent state is only conditioned by the initial prestress force of the cables (ρ), increasing the area of the cable-stayed system will not allow to further optimize the deck. As a result, the deck reaches its limit of optimization for $q_t/q_d = 0.50$. However, it should be noted that further optimization may still be possible by increasing the value of ρ.
- On the other hand, the area of the stays is conditioned by the stress variation caused by the variable loads. As a result, for values of q_t/q_d smaller than 0.50, although the deck cannot be further optimized, the area of the stays keeps increasing, resulting in less efficient designs.

In summary, based on the material quantities presented in Table 8.6, the optimal design is achieved for $q_t/q_d = 0.50$. This conclusion is further supported by Figure 8.11, which plots the degree of responsiveness versus the relative cost and carbon footprint (referenced to $q_t/q_d = 1.0$), based on the quantities provided in Table 8.5.

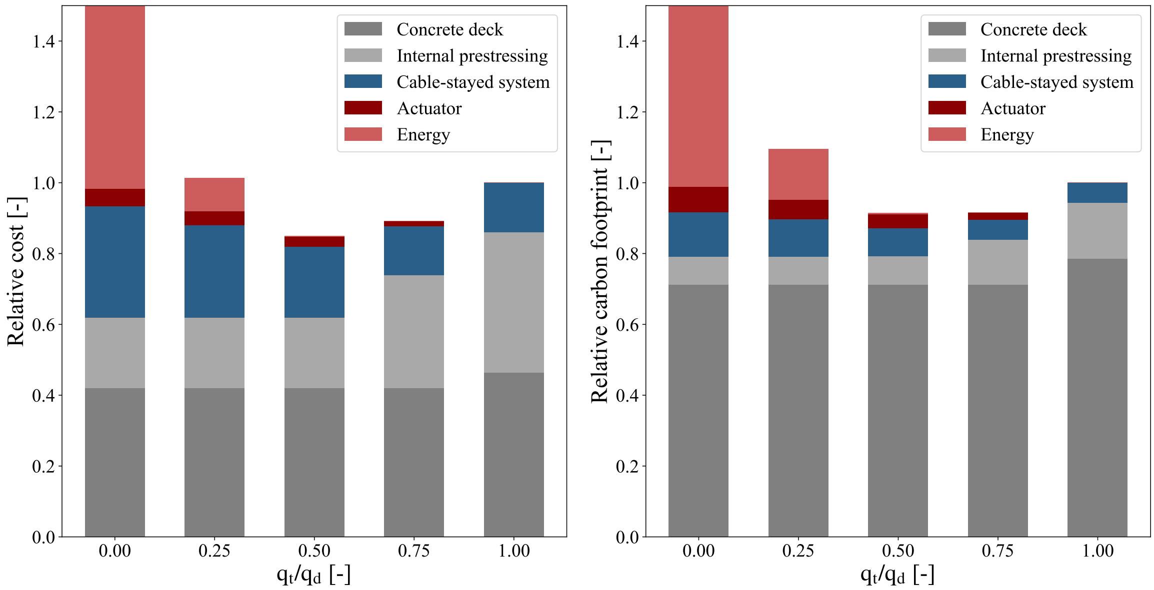

(a) Relative cost.

(b) Relative carbon footprint.

Figure 8.11: Comparison of the relative cost and carbon footprint for the optimized designs, with varying values of q_t/q_d.

Consistently, the optimal results are achieved for a ratio of $q_t/q_d = 0.50$, leading to a 15% reduction in costs and a 9% reduction in carbon emissions. However, it should be mentioned that certain design criteria established in the original project [91] have been maintained in this optimization. As will be discussed in the future research section, it shall be explored if modifications to these criteria can further optimize the system and make its implementation more viable.

Finally, it is worth noting that in this case, hydraulic actuators are chosen for their higher load capacity, but they come with the drawback of requiring significant energy consumption. On the other hand, in the case discussed in Chapter 6, electric actuators were employed. Despite the higher initial cost associated with electric actuators, they offer the advantage of lower energy costs. This is another reason why, in this study case, structures with low values of q_t/q_d become less competitive.

8.5 Conclusions

The structural response of a smart under-deck cable-stayed prestressed concrete bridge is studied, with the Osormort viaduct selected as the case study. The main findings of this research are:

- The analytical and numerical analyses of the Osormort viaduct confirm that the contribution of conventional under-deck cable-stayed systems in continuous bridges is mainly to the permanent state. In contrast, the efficiency of the system in withstanding live loads is low. This is due to the high stiffness of the concrete deck and, near the supports, to the low eccentricity of the cables.
- The application of the smart system to the case study demonstrates the effectiveness of this technology to reduce bending moments caused by traffic loads. This reduction is appreciated at midspan as well as near supports. The partially smart system is considered the optimal strategy for achieving a lower utilization factor along the whole deck.
- The improved efficiency achieved through the implementation of the smart system results in material savings on the deck, leading to both cost and emissions reductions. Specifically, the implementation of a partially smart system with a $q_t/q_d = 0.50$ results in a reduction in cost of up to 15% compared to the conventional viaduct. Additionally, this approach can achieve a 9% reduction in carbon emissions.

As a main conclusion, the implementation of a smart under-deck cable-stayed system in a full-scale bridge results in noteworthy structural enhancements. Nevertheless, the economic benefits appear to be less substantial than expected, which may question the widespread adoption of this technology in bridge construction. Further research and cost-benefit analysis are needed to determine the optimal scenarios for the implementation of this system.

Also, it is noted that these results are not comparable to those shown in Part II, where the smart system is applied to a footbridge, due to the differences of the structural typology and live-to-dead load ratios, among others.

In the analyses described in this chapter there are some factors that have been neglected. Although most of these aspects have been thoroughly analyzed in Part II, within the context of applying the smart system to a steel footbridge, and they are not expected to be a problem, they should be re-evaluated in the specific context of this different bridge typology to ensure that all requirements are still met. These aspects include the following:

- It should be ensured that the optimized structure is able to withstand the accidental scenarios of an actuator shutdown and a cable breakage.
- The dynamic behavior of the viaduct must be analyzed, especially considering the increased slenderness of the deck achieved through the smart system.

- The high compression forces acting on the deck may introduce stability problems, which should be verified.

Furthermore, it is likely that the results presented in Section 8.4.3 could be enhanced by exploring variations in certain aspects that have been unchanged with respect to the original project. Thus, the following additional actions could be taken:

- To perform a parametric analysis to determine the optimum value of the initial prestress force (factor ρ) when using the smart system.
- To investigate the option of using cables and anchorages designed for cable-stayed system instead of prestressing systems. Although they are more expensive, higher variations of tension in the stays can be reached. For the smart system to be really efficient, the cables have to be able to withstand high portions of the live load, so this modification would probably bring improved results.
- Another modification that could enhance the performance of cable-stayed systems in continuous bridges is to implement a combined cable-stayed system in the Osormort viaduct. This system, as indicated by Ruiz-Terán and Aparicio [97], involves a cable layout that passes from under the deck at midspan to over the deck at the supports, effectively increasing the efficiency of the system.

Part IV:

Conclusions

9

Conclusions

9.1 Conclusions

This thesis aimed to conduct a comprehensive study on smart under-deck cable-stayed structures, a novel structural typology where the behavior under live loads is enhanced by the combined use of the smart technology and cable-stayed systems. The integration of these two technologies gives the designer the ability to control the internal force distribution in the structure, leading to significant potential material savings.

The objective of this study is to investigate all the relevant aspects necessary to successfully design smart under-deck cable-stayed footbridges. This includes determining their optimum working procedure, analyzing their structural behavior, evaluating their impact in terms of cost and carbon emissions, and exploring various applications. In particular, the research encompasses the construction of a 6-meter-span footbridge prototype and the study of the system implementation into an existing road bridge, with the Osormort viaduct serving as a case study. By conducting a thorough investigation in these areas, this research provides the basis for designing smart under-deck cable-stayed systems, laying the groundwork for future developments.

Referring to the analytical and numerical study of a smart under-deck cable-stayed footbridge, the following conclusions can be drawn:

- The use of smart under-deck cable-stayed systems allows for a notable reduction in the material quantities. The numerical results show that the slenderness of the deck increases from $L/h = 28$ (no smart behavior considered) to a maximum of $L/h = 53$, resulting in a material reduction of approximately 35% on the deck. When following an analytical methodology, a maximum slenderness of $L/h = 57$ is achieved, indicating the consistency between both methodologies and validating the results.

- These optimal values ($L/h = 53$ and $L/h = 57$) are obtained for a partially smart structure with a degree of responsiveness of $q_t/q_d = 0.20$. This indicates that the actuator initiates its operation for any acting live load higher than 1 kN/m^2, equivalent to 20% of the design live load (q_d). For this value of q_t/q_d, although the design is governed by SLS, the material utilization factor (ULS) is also very high. This demonstrates that by forcing both limit states to be strictly fulfilled, it is possible to achieve a more optimized design.
- An extensive parametric analysis has revealed that smart systems are especially indicated when the live-to-dead load ratio is high, such as footbridges built with light materials. The optimum rise-to-span ratio is found between 0.10 and 0.20. Additionally, the optimal span is found between 25 and 75 m.
- It has been verified that the accidental situation of actuator failure, the vibration limit state, and the fatigue of the cables do not govern the design of the system, confirming the validity of the proposed design procedures.
- From an economic perspective, comparing a smart under-deck cable-stayed footbridge with its conventional equivalent reveals a cost savings of 13%. In terms of carbon footprint, there is a reduction of 23%, effectively highlighting the potential of smart structures to minimize the environmental impact of the construction industry.

Referring to the applications of the smart under-deck cable-stayed system, the following conclusions can be inferred:

- The experimental results, in terms of efficiency of the cable-stayed system, validate the analytical and numerical analysis.
- Several tests carried out on a 6-meter-span prototype have demonstrated that, when subjected to quasi-static loads, the smart system can significantly contribute to reduce the maximum deflection by up to 80% in the best case, compared to the deflection obtained without the smart system.
- Additionally, although the control has not been designed to directly improve the dynamic performance of the footbridge, it has been found that it allows to reduce the MTVV value up to 21.6% in the best-case scenario.

- The implementation of the smart under-deck cable-stayed system in the Osormort viaduct has revealed that, by adopting a partially smart strategy, it is possible to efficiently redistribute bending moments in the deck due to live load, which results in material savings.
- Specifically, for a partially smart system with $q_t/q_d = 0.50$, costs and carbon emissions could potentially be reduced by up to 15% and 9%, respectively, compared to the existing viaduct.

To summarize, the incorporation of smart under-deck cable-stayed systems in bridges leads to significant improvements in their structural performance. The smart system enables to intentionally redistribute the internal forces within the structure, based on the acting live load. By employing a partially smart strategy, each element of the structure can reach its maximum utilization level, allowing a substantial reduction in the required materials. The economic benefits attributed to the utilization of a partially smart under-deck cable stayed system amount to approximately 15% of the total bridge material cost. However, this outcome may be insufficient for promoting the widespread adoption of this technology in bridge construction. As a result, further research is necessary to explore strategies for enhancing the economic advantages of this system, thereby maximizing its potential and facilitating its integration into bridge construction practices.

9.2 Future research

There are several important directions for further research in this field, which are discussed next.

Generalization of the methodology

Firstly, as emphasized in the preceding sections of this thesis, it is important to acknowledge that the methods employed to obtain the aforementioned results have certain limitations. Therefore, to facilitate a more accurate evaluation of smart under-deck cable-stayed bridges, future research should prioritize the assessment of these weaknesses.

These aspects include the consideration of non-linear effects arising from both the geometry and the materials. Moreover, it should be determined whether the optimization process results in different outcomes if SLS in the deck is evaluated more precisely, specifically by directly calculating vibrations rather than relying on the simplified method of limiting deflections. In some specific cases, the integration of the smart system within the construction process should be analyzed.

Performing an exhaustive parametric analysis of various determinant aspects that have remained constant, such as the initial prestressing force or the number of struts, could enhance the design of the smart structure. Through the optimization of these parameters, it would be possible to achieve more material and cost-efficient bridges. Additionally, the study could lead to an improved understanding of the behavior of the system, which could ultimately be used to develop more robust design guidelines for smart under-deck cable-stayed structures. Moreover, it is important to study the utilization of alternative materials for the deck and the cables, such as fiber-reinforced polymers (FRP) instead of traditional steel cable-stayed systems.

Regarding the evaluation of the smart system, it is important to note that the analysis comparing the cost and carbon emissions of the smart system is limited in its scope, as it only considers the elements directly impacted by the system's implementation (deck and cable-stayed system). The analysis does not include other costs, such as sensors and the control system. In contrast, additional benefits of the smart system have not been accounted for in the analysis. For instance, the reduction in deck weight achieved through the implementation of the smart system results in lower loads on the substructure and auxiliary means (e.g. cranes), leading to significant cost savings. This aspect is of relevant significance in seismic areas. To get a complete evaluation of the overall economic and environmental impact of the smart system, a more holistic analysis that takes into account all costs and benefits should be performed. Maintenance and replacement considerations must also be taken into consideration.

Additionally, it is noted that the results have been obtained following a specific criterion based on maximizing the material utilization of the beam and the cable-stayed system. However, this solution is not necessarily the cheapest or most sustainable. Consequently, future research should be addressed to evaluate alternative design procedures to satisfy different optimization targets.

Regarding the experimentation, there are some critical areas that require improvement. First, the reduction of the response delay is essential to achieve better performance and a more stable response. Additionally, the system's robustness must be increased to ensure that it can withstand accidental situations, for which the prototype has not been tested. The scenario of different possible failures of the system has to be studied in detail before implementing the system into a real structure. In addition, it is necessary to assess the energy consumption of the smart system and explore different strategies to optimize it.

In relation to the control strategy, a primary focus of investigation should be directed towards defining a more refined and optimized control strategy. The experimental results would strongly benefit from incorporating a more sophisticated control strategy, such as a PI or PID control. This would allow to minimize the displacements in the deck and, consequently, the required structural material. In addition, it is important to note that the vibration reduction obtained with a smart control could be improved with a control law expressly designed to improve pedestrian comfort, for example, with velocity feedback.

On a bigger scale, the technology should be applied to a real-scale prototype (30-40 meters) to investigate aspects which have not been revealed in the 6-meter-span prototype. This would allow to test under more realistic pedestrian traffic conditions, which would provide more accurate insights of the limitations and advantages of the smart system. The constructive, economic, and functional limitations associated with increasing spans also need to be studied.

Furthermore, before implementing the proposed system in a real structure, it is crucial to thoroughly analyze several aspects that were not evaluated in this research due to its conceptual nature. For example, installing two parallel actuators should be considered, as it would allow to improve the behavior of the smart system when subjected to eccentric loads, as torsional effects could also be compensated. Other aspects include the evaluation of the accidental scenario concerning the breakage of a cable, considering its dynamic effect. In general, redundancy measures should be considered in the design, in the structural system (duplicating the cables) and in the smart system (introducing more actuators and sensors, planning strategies in case of power shortcuts, etc.), for future incorporation into a real structure.

In conclusion, all the factors mentioned above should be considered in future research efforts to improve the understanding and performance of smart under-deck cable-stayed footbridges. Further experimentation and testing is necessary to establish a comprehensive understanding of the behavior of these structures and promote their implementation in real-world applications. The measures described herein would enable the generalization of the proposed methodology, which is a necessary step towards the successful implementation of smart under-deck structures in practical design.

Discussion on reliability

In this work, the same reliability considerations that are indicated for conventional structures have been extrapolated to smart structures, (i.e., the safety factors and limit states defined in the Eurocodes are directly employed). However, the incorporation of mechanical components into the load-bearing structure, and their impact on the safety and reliability of the structure, should be considered. Before incorporating smart systems in real structures, it is necessary to investigate how current standards in civil engineering can be applied to smart structures or how they need to be extended in order to find the optimum balance between the reliability index of the structure and the consequences of a failure of the smart system. Ongoing research on adaptive structures has proposed alternative methods to achieve safe designs in these structures [98]–[100].

As indicated, directly applying the current codes does not sufficiently cover the requirements of smart structures, since the malfunction of the mechanical elements introduces different hazards and failure modes. These must be identified, analyzed, and incorporated into the design process. These particularities need to be taken into account when determining safety factors and load combination factors. Simplifications made in this work, such as treating the actuator failure as an Accidental Limit State (ALS), need to be reevaluated. These limit states, as considered in the Eurocodes, are associated with a probability of occurrence of the accidental event and a consequence of the failure. As with non-conventional accidental situations, a risk analysis must be done in order to establish the optimum design point, balancing the cost of improving the reliability index, the probability and consequences of the failure, as well as other sustainability indicators.

Ultimately, smart structures must be designed to ensure structural safety in the event of the failure of any of the components comprising the smart system. Therefore, their particularities should be integrated into the design process and the applied safety concept.

Extension to other structural typologies

To fully maximize the advantages of smart cable-stayed systems, it is crucial to investigate their potential application across various structural typologies. By expanding the utilization of these systems beyond the scope of this thesis, it may become possible to achieve greater benefits than the modest improvements observed on the analyzed footbridge.

For example, a promising application of smart cable-stayed systems is in the field of wind turbines. Currently, the towers of these structures are predominantly constructed using steel, but they often face limitations in height due to buckling, vibrations and fatigue concerns. As an alternative, concrete towers have emerged as a viable design option, since they do not have the same issues, although they face other challenges such as difficulties in transportation due to their increased weight. To maximize the advantages of concrete towers, they can be combined with a vertical cable-stayed system, which would allow the introduction of a circular uniform vertical compressive stress in the tube walls, effectively reducing tensile stresses under specific wind load conditions. By incorporating a smart system, the benefits of the cable-stayed system can be further enhanced, allowing to, for example, adjust the stiffness of the tower to the each stage (operation or extreme loading conditions). This approach would allow for a reduction in the required cross-section of the tower, minimizing the overall use of materials and reducing their weight. This technology would enable the possibility of constructing taller towers, allowing access to higher altitudes where stronger winds prevail.

Alternatively, vertical smart cable-stayed systems can be employed in lightweight façades, such as glass façades. In these structures, minimizing the weight of the primary element is crucial, and the incorporation of an external prestressed system can aid in withstanding wind loads while relieving stress on the main component. By equipping these elements with smart systems, the advantages of external prestressing can be further optimized.

On a different topic, some buildings with specialized applications, such as industrial factories and pharmaceutical laboratories, often have strict SLS requirements, while their ULS restrictions remain relatively normal. In such cases, rather than opting for excessively material-intensive slabs, the implementation of smart under-deck cable-stayed systems could prove to be a viable and cost-effective alternative.

Moveable bridges present another structural typology that can benefit from smart cable-stayed systems. These bridges experience varying load situations when changing from their “open position” to their “service position”. Lightweight structures provide a significant advantage during the open position, as they allow to reduce the size of the required mechanism to move the bridge. The application of a smart under-deck cable-stayed system has shown favorable results in reducing the material required for the deck, proving to be of potential use in these bridges. An additional advantage of this application is that movable bridges already incorporate mechanical components, so the additional cost of the smart system would be partially covered.

Finally, another possible research line would involve investigating the use of this technology for strengthening existing structures. Over time, certain structures such as bridges or industrial buildings are subjected to increased loads. Rather than considering extensive structural expansions, implementing a smart under-deck cable-stayed system could provide a viable solution to meet the growing demand for enhanced strength without requiring major construction efforts.

Bibliography

[1] D. P. Billington, “Historical Perspective on Prestressed Concrete,” *PCI Journal*, vol. 21, no. 5, pp. 48–71, 1976. DOI: 10.15554/pcij.09011976.48.71.

[2] International Federation for Structural Concrete (fib), “External Tendons for Bridges. State-of-the-art-report,” *FIB Bulletins*, vol. 97, 2020.

[3] M. Arici and M. F. Granata, “Conceptual design of prestressed slab bridges through one-way flexural load balancing,” *Structural Engineering and Mechanics*, vol. 48, pp. 615–642, 2013. DOI: 10.12989/sem.2013.48.5.615.

[4] A. M. Ruiz-Terán, “Unconventional Cable-stayed Bridges. Structural Behaviour and Design Criteria (Puentes atirantados no convencionales: comportamiento estructural y criterios de diseño),” (in Spanish), Ph.D. dissertation, Universidad de Cantabria, Santander, 2005, ISBN: 978-84-89670-68-6.

[5] D. Collings and A. S. Gonzalez, “Extradosed and cable-stayed bridges, exploring the boundaries,” *Proceedings of the Institution of Civil Engineers: Bridge Engineering*, vol. 166, no. 4, pp. 231–239, 2013. DOI: 10.1680/bren.10.00058.

[6] F. Sima and K. Stockhusen, “Evolution of cable-stayed bridges (Evolución de los Puentes Atirantados),” in *Cable Stayed and Extradosed Bridges - Conceptual Design and Structural Behaviour*, (in Spanish), 2014. DOI: http://dx.doi.org/10.13140/RG.2.2.30761.19045.

[7] A. Kasuga, “Extradosed bridges in Japan,” *Role of Concrete Bridges in Sustainable Development - Proceedings of the International Symposium - Celebrating Concrete: People and Practice*, pp. 17–30, 2003. DOI: 10.1680/rocbisd.32484.0002.

[8] J. A. Fernández Ordóñez, *Eugène Freyssinet*, 2nd ed. Cinter Divulgación Técnica, 2022.

[9] H. U. Aeberhard, P. Buergi, H. R. Ganz, P. Marti, P. Matt, and T. Sieber, “External Post-Tensioning - Design Considerations - VSL External Tendons - Examples from Practice,” *VSL Report Series*, 1992.

[10] J. J. Arenas de Pablo, "Bridges in Spain in the 20th century (Los puentes en España a lo largo del siglo XX)," *Revista de Obras Publicas*, vol. 146, no. 3388, pp. 176–184, 1999, (in Spanish).

[11] J. A. Lozano-Galant and I. Paya-Zaforteza, "Analysis of Eduardo Torroja's Tempul Aqueduct an important precursor of modern cable-stayed bridges, extradosed bridges and prestressed concrete," *Engineering Structures*, vol. 150, pp. 955–968, Nov. 2017. DOI: 10.1016/j.engstruct.2017.07.057.

[12] F. J. León González, *Notes for a History of Structural Concrete (Notas para una historia del hormigón estructural)*. 2021, (in Spanish), ISBN: 978-84-09-32530-6.

[13] *Structurae*, Accessed April 30, 2023. [Online]. Available: https://structurae.net/en.

[14] A. M. Ruiz Terán and A. C. Aparicio, "Developments in under-deck and combined cable-stayed bridges," *Proceedings of the Institution of Civil Engineers - Bridge Engineering*, vol. 163, no. 2, pp. 67–78, 2010. DOI: http://dx.doi.org/10.1680/bren.2010.163.2.67.

[15] A. M. Ruiz-Teran and A. C. Aparicio, "Parameters governing the response of under-deck cable-stayed bridges," *Canadian Journal of Civil Engineering*, vol. 34, no. 8, pp. 1016–1024, 2007. DOI: 10.1139/L07-016.

[16] A. Muttoni, "Some innovative prestressed concrete structures in Switzerland," *Keynote lecture at the 23rd Symposium on Developments in Prestressed Concrete*, p. 12, 2014.

[17] Unknown, "Neckar Valley Bridge, Weitingen (Neckartalbrücke, Weitingen)," *Schweizerische Bauzeitung*, vol. 96, no. 42, p. 797, 1978, (in German).

[18] A. Holgate, *The Art of Structural Engineering: The Work of Jorg Schlaich and His Team*. Edition Axel Menges, 1997, ISBN: 3930698676.

[19] J. Resplendino and J. Lefevre, "Under-deck prestressed bridge. Study of the structure nº13 on A 75 (Dalle précontrainte sousbandée. Etude de l'ouvrage d'art nº13 sur A 75)," *Bulletin Ouvrages d'Art (BOA)*, vol. 15, pp. 2–4, 1993, (in French).

[20] A. González, "Transversal axis of Catalonia. Calldetenes - Sant Juliá de Vilatorta - Sant Sadurní D'Osormort. (Eje transversal de Cataluña. Tramo: Calldetenes - Sant Juliá de Vilatorta - Sant Sadurní D'Osormort)," *Revista de Obras Públicas*, vol. 3364, pp. 61–66, May 1997, (in Spanish).

[21] M. Aguiló, J. Manterola, M. Onzain, and J. Rui-Wamba, *Javier Manterola Armisén. Philosophy and practice (Javier Manterola Armisén. Pensamiento y obra)*. Fundación ESTEYCO, 2004, (in Spanish), ISBN: 84-921092-7-0.

[22] European Committee for Standardization, *Eurocode 3: Design of steel structures*, 2019.

[23] Service d'Etudes Techniques des Routes et Autoroutes (SETRA), *Cable stays. Recommendations of French interministerial commission of prestressing*, 2002.

[24] Japan Prestressed Concrete Engineering Association. Publication committee for the English edition of Specifications for Design and Construction of Cable-Stayed Bridge and Extradosed Bridge, *Specifications for Design and Construction of Cable-Stayed Bridge and Extradosed Bridge*. 2011.

[25] International Association for Bridge and Structural Engineering (IABSE) - Working Commission 3, *Extradosed Bridges. State-of-the-Art-Report*, Jan. 2014.

[26] Asociación Española de Ingeniería Estructural (ACHE), *Recommendations and technical manuals. Structures and Building: Manual of Stays (Recomendaciones y manuales técnicos. Estructuras y Edificación: Manual de Tirantes (E–12))*, Colegio de Caminos, Canales y Puertos, Ed. 2007, (in Spanish), ISBN: 84-3800353-4.

[27] International Federation for Structural Concrete (fib), "Acceptance of stay cable systems using prestressing steels," *FIB Bulletins*, vol. 30, 2005.

[28] Post-Tensioning Institute (PTI), *Post-Tensioning Manual*, 6th ed. Phoenix, 2006, ISBN: 0-9778752-0-2.

[29] N. J. Gimsing and C. T. Georgakis, *Cable Supported Bridges: Concept and Design*, 3rd Edition. Wiley, 2012, ISBN: 978-0-470-66628-9.

[30] J. Ploch, "Definition of the Concept of Security in Prestressing (Zur Definition und zum Sicherheitskonzept der Vorspannung)," (in German), Ph.D. dissertation, Universität Stuttgart, 2004.

[31] T. D. Sterk, "Building upon Negroponte: A hybridized model of control suitable for responsive architecture," *Automation in Construction*, vol. 14, no. 2 SPEC. ISS, pp. 225–232, 2005. DOI: 10.1016/j.autcon.2004.07.003.

[32] *5 Smart Building Skins That Breathe, Farm Energy, and Gobble Up Toxins*, Accessed May 22, 2023. [Online]. Available: https://gizmodo.com/5-smart-building-skins-that-breathe-farm-energy-and-g-1254091559.

[33] *Moveables. sbp*, Accessed May 22, 2023. [Online]. Available: https://www.sbp.de/en/competencies/moveables/.

[34] *The Shed's Bloomberg Building*, Accessed May 22, 2023. [Online]. Available: https://theshed.org/about/building.

[35] T. Soong, "Active structural control in civil engineering," *Engineering Structures*, vol. 10, pp. 74–84, 1988. DOI: 10.1016/0141-0296(88)9033-8.

[36] *Adaptive structures. Institute for Lightweight Structures and Conceptual Design. University of Stuttgart*, Accessed May 27, 2023. [Online]. Available: https://www.ilek.uni-stuttgart.de/en/research/adaptive-structures/.

[37] W. Sobek and P. Teuffel, "Adaptive systems in architecture and structural engineering," in *Smart Structures and Materials 2001: Smart Systems for Bridges, Structures, and Highways*, S.-C. Liu, Ed., International Society for Optics and Photonics, vol. 4330, SPIE, 2001, pp. 36–45. DOI: 10.1117/12.434141.

[38] W. Sobek, A. Weilandt, and C. Lemaitre, "Topology of Adaptive Lightweight Structures," *IASS-APCS Symposium New Olympics, New Shell and Spatial Structures*, 2006.

[39] W. Sobek, P. Teuffel, A. Weilandt, and C. Lemaitre, "Adaptive and Lightweight," in *Adaptables2006, TU/e, International Conference on Adaptable Building Structures*, 2006, pp. 6-38 –6-42.

[40] J. Hunt, W. Haase, and W. Sobek, "Designing Adaptive Spatial Structures," *Journal of the International Association for Shell and Spatial Structures*, 2008.

[41] O. Sawodny, M. Weickgenannt, S. Neuhaeuser, and W. Sobek, "Active Vibration Control of a Double-Curved Shell Structure Using the example of Stuttgart Smartshell," *Proceedings of the ASME 2012 International Mechanical Engineering Congress and Exposition*, 2012.

[42] W. Sobek, "Ultra-lightweight construction," *International Journal of Space Structures*, vol. 31, no. 1, pp. 74–80, 2016. DOI: 10.1177/0266351116643246.

[43] M. Woerner, M. Weickgenannt, S. Neuhaeuser, C. Goehrle, W. Sobek, and O. Sawodny, "Kinematic modeling of a hydraulically actuated 3-SPR-parallel manipulator for an adaptive shell structure," *2013 IEEE/ASME International Conference on Advanced Intelligent Mechatronics: Mechatronics for Human Wellbeing, AIM 2013*, pp. 1330–1336, 2013. DOI: 10.1109/AIM.2013.6584279.

[44] R. van Bommel, A. Habraken, and P. Teuffel, "Adaptive arch: Active stress minimization in a thin arch structure," *Procedia Engineering*, vol. 155, pp. 265–274, 2016. DOI: https://doi.org/10.1016/j.proeng.2016.08.028.

[45] L. Blandini, W. Haase, S. Weidner, *et al.*, "D1244: Design and construction of the first adaptive high-rise experimental building," English, *Frontiers in Built Environment*, vol. 8, Jun. 2022. DOI: 10.3389/fbuil.2022.814911.

[46] *D1244 - The world's first adaptive skyscraper*, Accessed May 27, 2023. [Online]. Available: https://www.sfb1244.uni-stuttgart.de/en/.

[47] A. Bleicher, M. Schlaich, Y. Fujino, and T. Schauer, “Model-based design and experimental validation of active vibration control for a stress ribbon bridge using pneumatic muscle actuators,” *Engineering Structures*, vol. 33, no. 8, pp. 2237–2247, 2011. DOI: 10.1016/j.engstruct.2011.02.035.

[48] A. Bleicher, T. Schauer, M. Valtin, J. Raisch, and M. Schlaich, “Active vibration control of a light and flexible stress ribbon footbridge using pneumatic muscles,” *IFAC Proceedings Volumes*, vol. 44, no. 1, pp. 911–916, 2011, 18th IFAC World Congress. DOI: https://doi.org/10.3182/20110828-6-IT-1002.02781.

[49] A. Bleicher, M. Schlaich, and T. Schauer, “Multimodal and multivariable active vibration control for a footbridge – model-based design and experimental validation,” 2011.

[50] F. A. dos Santos and C. Cismaşiu, “Adaptive underslung beam using shape-memory alloys for frequency-tuning,” *Journal of Intelligent Material Systems and Structures*, vol. 28, no. 10, pp. 1260–1271, 2017. DOI: 10.1177/1045389X16667558.

[51] Q. Wang, G. Senatore, K. Jansen, A. Habraken, and P. Teuffel, “Design and characterization of variable stiffness structural joints,” *Materials and Design*, vol. 187, p. 108 353, 2020. DOI: https://doi.org/10.1016/j.matdes.2019.108353.

[52] G. Senatore, P. Duffour, and P. Winslow, “Synthesis of minimum energy adaptive structures,” *Structural and Multidisciplinary Optimization*, vol. 60, pp. 849–877, 2019. DOI: 10.1007/s00158-019-02224-8.

[53] A. P. Reksowardojo, G. Senatore, A. Srivastava, C. Carroll, and I. F. Smith, “Design and testing of a low-energy and-carbon prototype structure that adapts to loading through shape morphing,” *International Journal of Solids and Structures*, p. 111 629, 2022. DOI: https://doi.org/10.1016/j.ijsolstr.2022.111629.

[54] G. Senatore, P. Duffour, P. Winslow, and C. Wise, “Shape control and whole-life energy assessment of an ‘infinitely stiff’ prototype adaptive structure,” *Smart Materials and Structures*, vol. 27, no. 1, p. 015 022, 2017. DOI: 10.1088/1361-665x/aa8cb8.

[55] G. Senatore, P. Duffour, S. Hanna, P. Winslow, and C. Wise, “Designing adaptive structures for whole life energy savings,” *Research and Applications in Structural Engineering, Mechanics and Computation*, no. April 2014, pp. 2105–2110, 2013. DOI: 10.1201/b15963-380.

[56] T. Noack, J. Ruth, and U. Muller, “Adaptive hybrid structures,” *Proceedings of the international conference on adaptable building structures, Adaptables*, pp. 9–256 – 9–260, 2006.

[57] A. W. Nicklisch, *Adaptively Prestressed Concrete Structures*, Master thesis. Massachusetts Institute of Technology, 2000.

[58] S. Kmet, V. Urban, M. Tomko, and R. Soltys, "Analisis of an adaptive tensegrity module," in *IASS Symposium 2019*, International Association for Shell and Spatial Structures (IASS), 2019, pp. 121–128.

[59] B. Adam and I. F. Smith, "Active tensegrity: A control framework for an adaptive civil-engineering structure," *Computers and Structures*, vol. 86, no. 23-24, pp. 2215–2223, 2008. DOI: 10.1016/j.compstruc.2008.05.006.

[60] P. Pacheco and A. Adao Da Fonseca, "Effector systems in structures.," *Conceptual design of structures – Proceedings of IASS Symposium, Stuttgart*, pp. 339–346, 1996.

[61] P. Pacheco, *Gantry with auto-adjusting prestressing*. World Intellectual Property Organization. WO 2004/109018 A1, 2004.

[62] P. Pacheco and A. M. Adão da Fonseca, "Organic Prestressing," *Journal of Structural Engineering*, vol. 128, no. 3, pp. 400–405, Mar. 2002. DOI: 10.1061/(ASCE)0733-9445(2002)128:3(400).

[63] G. Senatore, P. Duffour, and P. Winslow, "Exploring the application domain of adaptive structures," *Engineering Structures*, vol. 167, pp. 608–628, 2018. DOI: 10.1016/j.engstruct.2018.03.057.

[64] P. Pacheco, A. Guerra, P. Borges, and H. Coelho, "A scaffolding system strengthened with organic prestressing - The first of a new generation of structures," *Structural Engineering International: Journal of the International Association for Bridge and Structural Engineering (IABSE)*, vol. 17, no. 4, pp. 314–321, 2007. DOI: 10.2749/101686607782359092.

[65] M. Crusells-Girona and A. C. Aparicio, "Active control implementation in cable-stayed bridges for quasi-static loading patterns," *Engineering Structures*, vol. 118, pp. 394–406, 2016. DOI: https://doi.org/10.1016/j.engstruct.2016.03.061.

[66] F. Ferreira and L. Simões, "Optimum design of a controlled cable-stayed footbridge subject to a running event using semiactive and passive mass dampers," *Journal of Performance of Constructed Facilities*, vol. 33, Jun. 2019. DOI: 10.1061/(ASCE)CF.1943-5509.0001285.

[67] A. P. Reksowardojo, G. Senatore, L. Blandini, and M. Bischoff, "Vibration Control of Simply Supported Beam Bridges Equipped with an Underdeck Adaptive Tensioning System," in *IABSE Congress: Bridges and Structures: Connection, Integration and Harmonisation*, Nanjing, China, 2022, pp. 539–548.

[68] United Nations Environment Program, *2022 global status report for buildings and construction: Towards a zero-emission, efficient and resilient buildings and construction sector*, Nairobi, 2022.

[69] G. Feltrin, J. Meyer, W. Boyle, *et al.*, "Monitoring Instrumentation and Techniques - Background Document," *Sustainable Development*, p. 136, 2007.

[70] P. Regtien and E. Dertien, "6 - inductive and magnetic sensors," in *Sensors for Mechatronics (Second Edition)*, P. Regtien and E. Dertien, Eds., Second Edition, Elsevier, 2018, pp. 145–182, ISBN: 978-0-12-813810-6. DOI: https://doi.org/10.1016/B978-0-12-813810-6.00006-9.

[71] M. Weickgenannt, S. Neuhaeuser, B. Henke, W. Sobek, and O. Sawodny, "Optimal sensor placement for state estimation of a thin double-curved shell structure," *Mechatronics*, vol. 23, no. 3, pp. 346–354, 2013. DOI: 10.1016/j.mechatronics.2013.01.009.

[72] B. Douglas, *The Fundamentals of Control Theory An Intuitive Approach from the Creator of Control System Lectures on YouTube.* 2019. [Online]. Available: http://creativecommons.org/licenses/by-nc-sa/4.0..

[73] G. Senatore, P. Duffour, S. Hanna, F. Labbé, and P. Winslow, "Adaptive structures for whole-life energy savings," *Journal of the International Association for Shell and Spatial Structures*, vol. 52, no. 170, pp. 233–240, 2011. DOI: 10.1109/IE.2011.40.

[74] P. H. Kirkegaard and D. Parigi, "On Control Strategies for Responsive Architectural Structures," *ASS- APCS 2012 Proceedings: from spatial structures to space structures. The International Association for Shell and Spacial Structures.*, p. 8, 2012.

[75] Motion control tips, *How to select a pneumatic actuator: An engineer's guide*, Accessed May 28, 2023. [Online]. Available: https://www.motioncontroltips.com/selecting-a-pneumatic-actuator/.

[76] L. Todisco, H. Corres, and C. Mueller, "Funicularity through External Posttensioning: Design Philosophy and Computational Tool," *Journal of Structural Engineering*, vol. 142, no. 2, p. 04 015 141, 2016. DOI: 10.1061/(asce)st.1943-541x.0001416.

[77] European Committee for Standardization, *Eurocode 0: Basis of structural design*, 2019.

[78] European Committee for Standardization, *Eurocode 1: Actions on structures*, 2019.

[79] European Commission, Directorate-General for Research and Innovation, M. Feldmann, C. Heinemeyer, and M. Lukić, *Human-induced vibration of steel structures (Hivoss)*. Publications Office, 2010. DOI: doi/10.2777/79056.

[80] A. M. Ruiz-Teran and A. C. Aparicio, "Structural behaviour and design criteria of under-deck cable-stayed bridges and combined cable-stayed bridges. Part 1: Single-span bridges," *Canadian Journal of Civil Engineering*, vol. 35, no. 9, pp. 938–950, 2008. DOI: 10.1139/L08-033.

[81] London Energy Transformation Initiative (LETI), *Embodied Carbon Primer*, 2020.

[82] The Institution of Structural Engineers, *How to calculate embodied carbon*, London, 2020. [Online]. Available: www.istructe.org.

[83] *Smart Cable-Stayed Footbridge by UPM, Spain*, Accessed May 13, 2023. [Online]. Available: https://vimeo.com/726758617.

[84] J. Soria, I. M. Díaz, J. H. García-Palacios, and N. Ibán, "Vibration monitoring of a steel-plated stress-ribbon footbridge: Uncertainties in the modal estimation," *Journal of Bridge Engineering*, vol. 21, no. 8, p. C5015002, 2016. DOI: https://doi.org/10.1061/(ASCE)BE.1943-5592.0000830.

[85] B. Peeters and G. De Roeck, "Reference-based stochastic subspace identification for output-only modal analysis," *Mechanical Systems and Signal Processing*, vol. 13, no. 6, pp. 855–878, 1999. DOI: https://doi.org/10.1006/mssp.1999.1249.

[86] S. Živanović, A. Pavic, and P. Reynolds, "Vibration serviceability of footbridges under human-induced excitation: A literature review," *Journal of sound and vibration*, vol. 279, no. 1-2, pp. 1–74, 2005. DOI: https://doi.org/10.1016/j.jsv.2004.01.019.

[87] S. Živanović, "Benchmark footbridge for vibration serviceability assessment under vertical component of pedestrian load," *Journal of Structural Engineering*, vol. 138, no. 10, pp. 1193–1202, 2012. DOI: https://doi.org/10.1061/(ASCE)ST.1943-541X.0000571.

[88] ISO 10137, *Bases for design of structures – serviceability of buildings and walkways against vibrations*, International Organization for Standardization, 2007.

[89] ISO 2631–1, *Mechanical vibration and shock: Evaluation of human exposure to whole-body vibration. part 1, general requirements*, International Standard, 1997.

[90] F. Tubino and G. Piccardo, "Serviceability assessment of footbridges in unrestricted pedestrian traffic conditions," *Structure and Infrastructure Engineering*, vol. 12, no. 12, pp. 1650–1660, 2016. DOI: 10.1080/15732479.2016.1157610.

[91] J. Manterola-Armisén and L. Fernández-Troyano, *Osormort viaduct. Project (Viaducto de Osormort. Proyecto).* (in Spanish), May 1993.

[92] *Carlos Fernández Casado S.L.* Accessed April 30, 2023. [Online]. Available: https://www.cfcsl.com.

[93] Ministerio de Fomento, *Instruction on actions to be considered in the design of road bridges (IAP–72) (instrucción relativa a las acciones a considerar en el proyecto de puentes de carreteras (IAP–72))*, (in Spanish), 1972.

[94] Ministerio de Fomento, *Instruction for the design and execution of works of mass or reinforced concrete (EH–91) (instrucción para el proyecto y la ejecución de obras de hormigón en masa o armado (EH–91))*, (in Spanish), 1991.

[95] L. Todisco, H. Corres, A. Caldentey, A. Addante, and J. Cañada, "Conceptual design of spatial arch footbridges supporting curved decks," *Structures*, vol. 33, pp. 1207–1215, Oct. 2021. DOI: 10.1016/j.istruc.2021.05.003.

[96] J. Strasky, "The Power of prestressing," *Structural Concrete*, vol. 4, no. 1, pp. 25–42, 2003. DOI: 10.1680/stco.4.1.25.38234.

[97] A. M. Ruiz-Teran and A. C. Aparicio, "Structural behaviour and design criteria of under-deck cable-stayed bridges and combined cable-stayed bridges. Part 2: Multispan bridges," *Canadian Journal of Civil Engineering*, vol. 35, no. 9, pp. 951–962, 2008. DOI: 10.1139/L08-034.

[98] *Methods and technologies for fail-safe elements and frameworks of adaptive load-bearing structures*, Accessed June 4, 2023. [Online]. Available: https://www.ibb.uni-stuttgart.de/en/research/sfb1244-b03/.

[99] D. Efinger, A. Ostertag, M. Dazer, D. Borschewski, S. Albrecht, and B. Bertsche, "Reliability as a key driver for a sustainable design of adaptive load-bearing structures," *Sustainability*, no. 14(2), 2022. DOI: 10.3390/su14020895.

[100] M. Dazer, A. Ostertag, T. Herzig, D. Borschewski, S. Albrecht, and B. Bertsche, "Consideration of reliability and sustainability in mechanical and civil engineering design to reduce oversizing without risking disasters," presented at the LCM 2021 (10th International Conference on Life Cycle Management) (Stuttgart), 2021.